THE EFFECT OF ANNEALING REGIME ON THE PRECIPITATION OF $FeCoNiAl_{0.75}Nb_{0.25}$ HIGH ENTROPY ALLOY

Minh Duc Le[1,2,*], Thanh Hung Nguyen[1], Manh Hung Nguyen[1], Hong Hai Nguyen[2]

[1]*Faculty of Mechanical Engineering, Le Quy Don Technical University*

[2]*School of Materials Science and Engineering, Hanoi University of Science and Technology*

Abstract

This paper investigates the effect of the annealing regime on the precipitation of $FeCoNiAl_{0.75}Nb_{0.25}$ high entropy alloy. The as-cast microstructure consists of coarse dendritic phases that are replaced by equiaxed morphology, and the distribution of the interdendritic phase becomes regularly better with increasing time and annealing temperature up to 825ºC. The precipitated process begins at 700ºC for 8 hours, shortening to 4 hours when the annealing temperature increases. The size of this phase is only a few μm. The fraction of the precipitated phase increases and the size of the dendritic phase is reduced as the annealing temperature is up to 825ºC, while this size rises in the 925ºC/16 hours regime. The microstructure is coarse, and the precipitated phase gradually disappears when the annealing is at 1000ºC. The HV3 hardness of the alloy increases with annealing time when the temperature is lower than 825ºC and reaches the highest value of ~ 614 kg/mm^2 at 600ºC/ 24 hours; this value begins to decrease for the 925ºC/16 hours regime. Meanwhile, the hardness gradually decreases with increasing annealing time at 1000ºC. It can be expected due to the rapid coarsening of the dendritic phase, the decrease in the proportion of the precipitated phase in the alloy, and the appearance of plastic flow phenomena at grain boundaries.

Keywords: *High entropy alloy; $FeCoNiAl_{0.75}Nb_{0.25}$ alloy; annealing; precipitation process.*

1. Introduction

High-entropy alloys are composed of at least five elements with equivalent composition according to the definition first given by Yeh *et al.* [1]. This alloy has been researched extensively because of its superior properties to traditional alloys, such as high hardness, and good wear resistance [2], and the ability to work well in high and low-temperature regions [3-6]. These properties are determined by the component design and the formed microstructure. The elemental composition of HEA is based on transition elements such as Co, Cr, Fe, Co, and Ni and supplemented with other elements such as Al, Cu, V, Mn, Ti, Nb and Mo [1, 7-19]. Adding Al and Nb to the FeCoNi base alloy has shown excellent mechanical properties [20-23]. Meanwhile, the microstructure in the as-cast state of the alloy is predicted through thermodynamic

* Corresponding author email: duclm@lqdtu.edu.vn
DOI: 10.56651/lqdtu.jst.v2.n02.848.pce

parameters such as the mixing entropy (ΔS_{mix}), the enthalpy of mixing (ΔH_{mix}), difference in atomic size (δ), valence electron concentration (VEC), and Ω criterion [19, 24]. Heat treatment can significantly change the microstructure of HEA and directly affect their properties [25-29].

However, a complete study has not been done on the influence of annealing on the microstructure of FeCoNiAlNb-based alloys. Therefore, this article studies the structural changes of equiatomic $FeCoNiAl_{0.75}Nb_{0.25}$ alloy according to annnealing temperature and time. As a basis for future research and applications of this alloy.

2. Experimental procedure

$FeCoNiAl_{0.75}Nb_{0.25}$ alloy is melted from pure metals (Fe, Co, Ni, Al, Nb) with purity over 99.9% in a vacuum induction furnace in a high-purity argon environment and poured into a water-cooled copper mold. The cast ingot has dimensions of about 80 × 25 × 15 mm^3 (Fig. 1). The composition of the cast ingot was determined by energy dispersive X-ray spectroscopy (EDX) as shown in Table 1. Annealing samples of size 5 × 5 × 5 mm^3 were carried out at: 600, 700, 825, 925, 1000ºC for 4, 8, 16, and 24 hours. The samples were ground to × 2000 silicon carbide paper, polished to completely remove scratches and etched with aqua regia solution (ratio HNO_3:HCl = 1:3) for 1 minute.

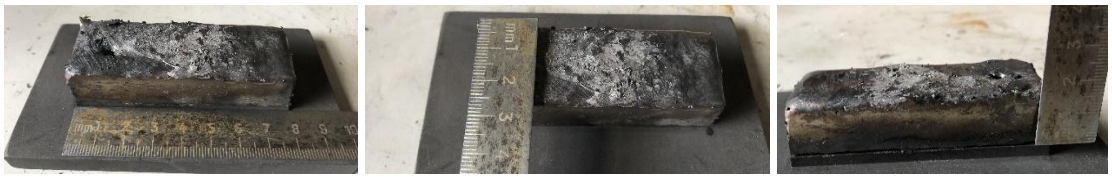

Fig. 1. Dimensions of $FeCoNiAl_{0.75}Nb_{0.25}$ alloy ingot after casting.

Using a combination of an Axiovert A2M optical microscope, a Jeol JSM-IT200 scanning electron microscope (SEM), and an Aeris X-ray diffraction equipment with Cu K radiation to study the alloy's microstructure. Vicker hardness (HV3) measurements were performed five times on each sample to obtain an average value under a load of 3 kg for 15 seconds on a Wilson Wolpert instrument.

Table 1. Chemical composition of bulk as-cast $FeCoNiAl_{0.75}Nb_{0.25}$ HEA (wt.%)

Element	**Fe**	**Co**	**Ni**	**Al**	**Nb**
Calculated composition	25.74	27.17	27.05	9.33	10.71
Actual composition	27.20	27.59	25.11	8.97	11.13

3. Results and discusstion

3.1. The as-cast microstructure

Figure 2 shows the as-cast microstructure of the alloy. The microstructure is characterized by large and coarse dendrites, the length of which can be up to hundreds μm, while the secondary dendrite arm spacing is only about ten μm. Interspersed is small and fine interdendrite unevenly distributed. Its size is only a few μm.

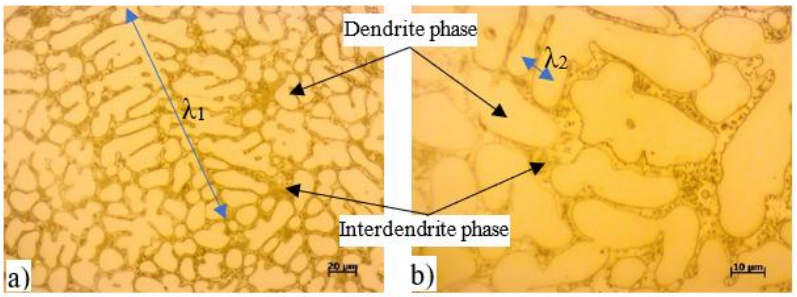

Fig. 2. The as-cast microstructure: a) ×200, b) ×500.

3.2. The annealed microstructure for 4 hours at different temperatures

Figure 3 shows the microstructure of the $FeCoNiAl_{0.75}Nb_{0.25}$ alloy samples after annealing at 600, 700, 825, 925, and 1000°C for 4 hours. As the annealing temperature increases, the dendrite structure gradually disappears and is replaced by equiaxial grains, and the interdendritic phase becomes more evenly distributed.

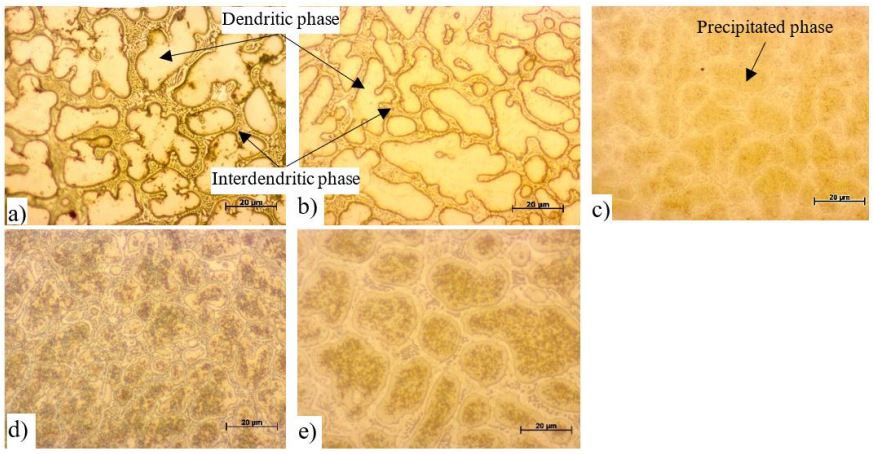

Fig. 3. The annealed micro-structure for 4 hours at: a) 600°C, b) 700°C, c) 825°C, d) 925°C, e) 1000°C. ×500.

At 825°C (Fig. 3c), a significant change in the dendrite phase is observed, with the precipitation of a finely dispersed phase in the initial inter-dendritic phase. This transformation is further accentuated at 925 and 1000°C, where the initial dendrite

phase becomes more equiaxial. However, the size of the dendritic phase also increases notably at 1000°C.

3.3. The annealed microstructure for 8 hours at different temperatures

When annealed for 8 hours, the dendritic phase was more uniform, and the inter-dendritic phase was more evenly distributed after annealing at 600°C (Fig. 4a); the precipitated phase appeared in the matrix at 700°C (Fig. 4b). The microstructure was almost unchanged when performed at 825 and 925°C compared to the case of annealing for 4 hours. Meanwhile, the precipitated phase decreased after annealing at 1000°C (Fig. 4e).

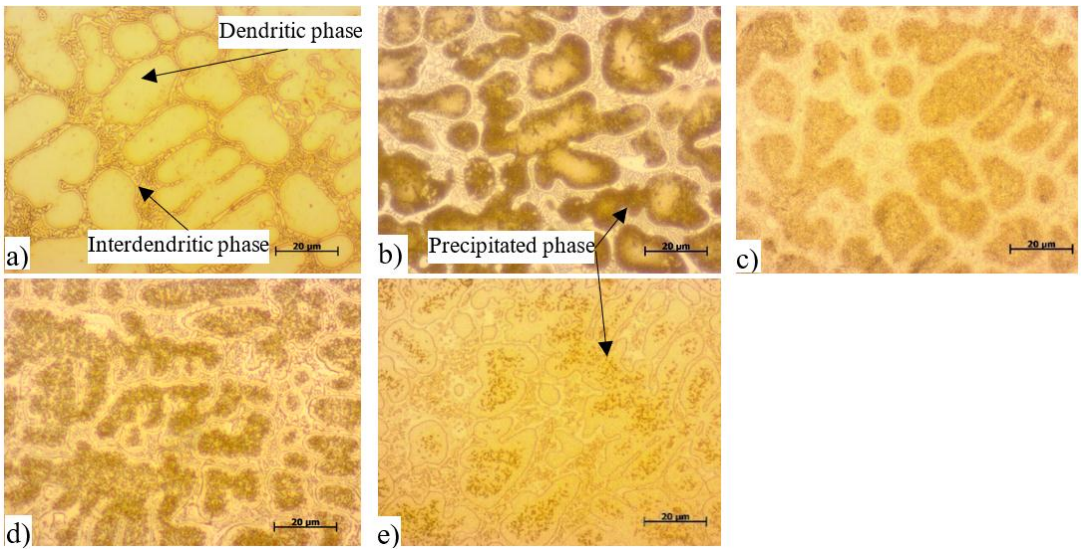

Fig. 4. The annealed microstructure for 8 hours at: a) 600°C, b) 700°C, c) 825°C, d) 925°C, e) 1000°C. ×500.

3.4. The annealed microstructure for 16 hours at different temperatures

Figure 5 shows the microstructure images of the alloy annealed for 16 hours at different temperatures. The size of the dendritic phase decreased at 600°C and 700°C, and the distance between these phases also decreased significantly, making their distribution more uniform.

At 600°C (Fig. 5a), no precipitation was observed in the matrix phase, a stark contrast to the significant increase in the amount of precipitated phase at 700°C (Fig. 5b). The phase morphology remained relatively unchanged at 825ºC (Fig. 5c). However, as the temperature approached 925°C, the fraction of the precipitated phase notably decreased (Fig. 5d), and the dendrite phase size increased at 1000°C (Fig. 5e).

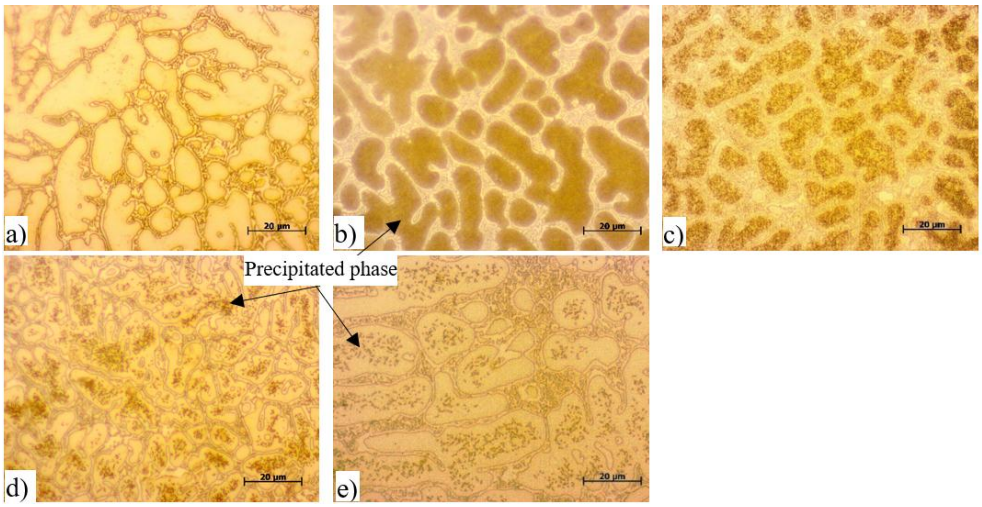

Fig. 5. The annealed microstructure for 16 hours at: a) 600°C, b) 700°C, c) 825°C, d) 925°C, e) 1000°C. ×500.

3.5. The annealed microstructure for 24 hours at different temperatures

The results after annealing for 24 hours in Fig. 6 show that the precipitated phase almost does not appear at 600°C. This phase's morphology and fraction remained virtually unchanged at 700°C and 825°C. Meanwhile, the size of the dendritic phase increased significantly in the case of annealing at 925°C and 1000°C. Almost no previously precipitated phase was observed in the case of incubation at 1000°C.

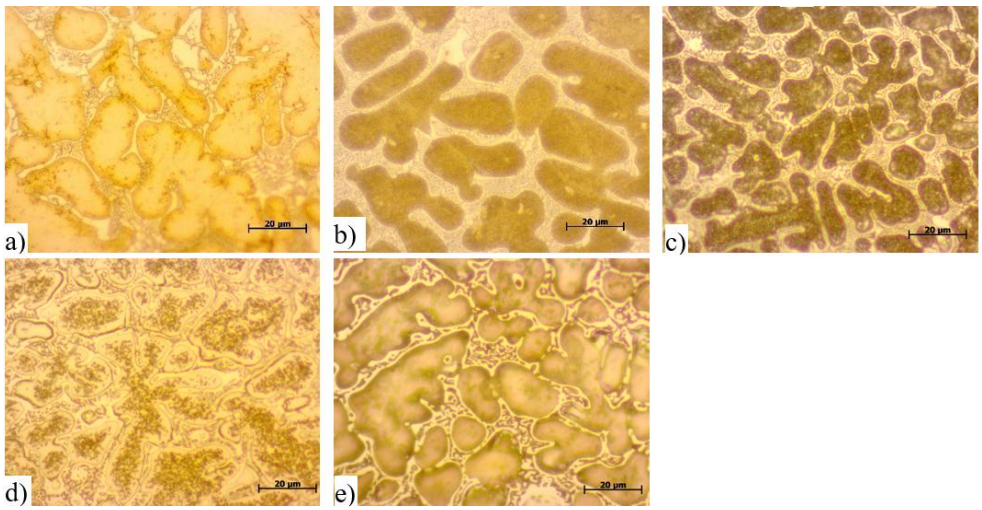

Fig. 6. The annealed microstructure for 24 hours at: a) 600° C, b) 700 °C, c) 825 °C, d) 925 °C, e) 1000 °C. ×500.

Based on the SEM image of the alloy in Fig. 7, it can be seen that the structure after annealing at 600ºC/24 hours is similar to the as-cast structure (Fig. 7a). However,

the dendritic phase becomes more equiaxial, and the interdendritic phase has a morphology similar to a eutectic-like structure [20] distributed more evenly (Fig. 7b). No precipitation was observed in the matrix phase - Fig. 7b. When annealing at 825ºC, the phase precipitation in the matrix occurs intensely, and the size of this phase is only about 1-2 µm. This phase exists very little when increasing the temperature to 1000ºC. The interdendritic phase changes from a eutectic-like morphology to a mesh surrounding the dendritic phase, on which deep grooves begin to appear at 825ºC; this groove size increases, and there is a plastic flow phenomenon at the grain boundaries when increasing the temperature to 925ºC for 16 hours.

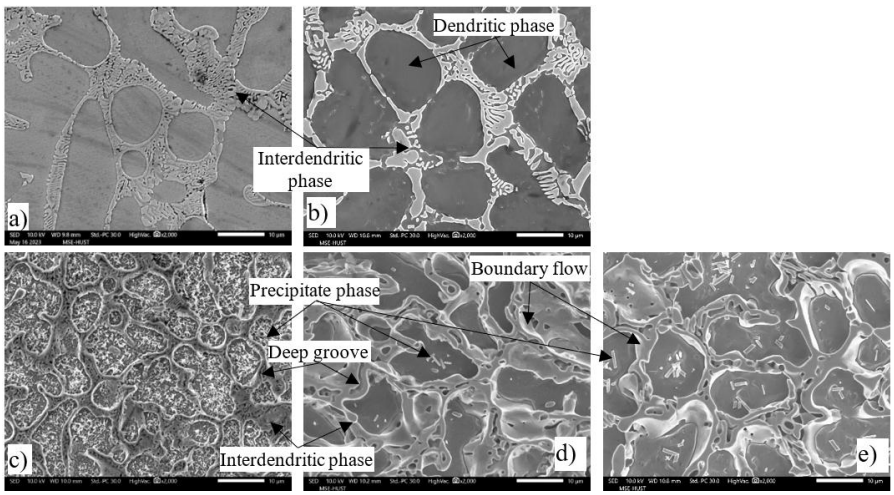

Fig. 7. SEM images: a) as-cast state; annealed for 24 hours at: b) 600°C, c) 825°C, d) 1000°C, and e) 925°C for 16 hours. ×2000.

3.6. Determine phase

The formation of phases in high-entropy alloys can be predicted by thermodynamic parameters, including the difference in atomic size (δ), the enthalpy of mixing (ΔH_{mix}), the entropy of the process mixing (ΔS_{mix}), valence electron concentration (VEC), and Ω criterion. For the $FeCoNiAl_{0.75}Nb_{0.25}$ alloy system, the values of these parameters after calculation are listed in Table 2.

The XRD analysis results in Fig. 8 show that in the as-cast state, the alloy exists as a phase mixture of FCC + BCC + IM [20, 23, 31], consistent with the thermodynamic calculation results in Table 2. The diffraction peak of the BCC phase has the most vigorous intensity, showing that it plays the role of the matrix phase in the microstructure. The ratio of the intermetallic phase and FCC is relatively small. The precipitation process is most clearly shown when annealing at 825°C. The heating time is up to 8 hours; the BCC phase ratio remains almost the same (constant intensity), and

a part of the BCC phase transforms into the FCC phase (peak 2θ = 43.7°). The diffraction peak appears at 2θ = 37.7° corresponding to the intermetallic phase (Laves) [20, 23]. When the annealing time was increased to 24 hours, the amount of intermetallic phase increased, especially at the diffraction peak corresponding to the BCC phase; an additional peak of the intermetallic phase also appeared, consistent with the SEM results above.

Table 2. Thermodynamic parameters of the alloy

Parameters	**Solid solution formation value**	**Calculated value**	**Phase in this work**
$\Delta H_{mix} = \sum_{i=1,i\#j}^{N} 4\Delta H_{AB}^{mix} c_i c_j$	-15 < ΔH_{mix} < 5 (kJ/mol) [19]	-15.78	FCC + BCC + IM
$\Delta S_{mix} = -R\sum_{i=1}^{n} c_i \ln c_i$	11 ≤ ΔS_{mix} ≤ 19.5 (J/K mol) [24]	12.7	
$\delta = 100\sqrt{\sum_{i=1}^{N} c_i\left(1-\frac{r_i}{\bar{r}}\right)^2}$	δ ≤ 6.6 % [24]	6.2	
$\Omega = \frac{T_m \Delta S_{mix}}{\lvert\Delta H_{mix}\rvert}$	Ω > 1.1 [24]	1.35	
$VEC = \sum_{i=1}^{n} c_i (VEC)_i$	VEC ≥ 8.0: (FCC); VEC ≤ 6.87: (BCC); 6.87 < VEC < 8.0: (BCC + FCC). HEAs contain Ti, Nb, V…6.88 ≤ VEC ≤ 7.84 tend to form σ phase (IM) [18, 30]	7.63	
where r_i is the Goldschmidt atomic radius of the i^{th} element, c_i is the molar ratio and ΔH_{ij}^{mix} is the mixing enthalpy between the i^{th} and j^{th} elements, T_m is the average melting temperature, $(VEC)_i$ valence electron concentration of element i and R (= 8.314 J/K.mol) is the gas constant. - FCC is face-centered cubic; BCC is body-centered cubic; IM is intermetallic.			

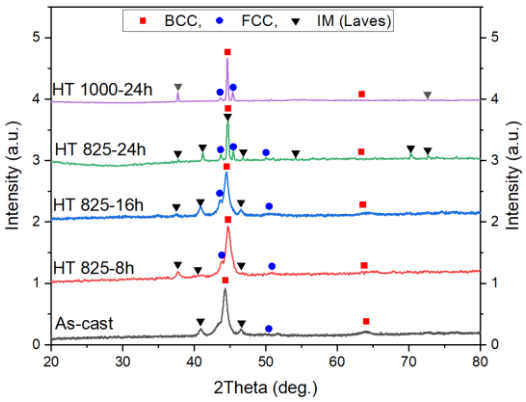

Fig. 8. XRD analysis results.

When the annealing temperature increased to 1000ºC, the proportion of the BCC phase increased, while the proportion of the intermetallic phase decreased clearly, and additional diffraction peaks corresponding to the FCC phase appeared [20, 23, 31]. This may be because the high-entropy effect significantly reduces the Gibbs free energy of the system [1], which quickly creates the formation of solid solutions during solidification rather than ordered compounds, especially at high temperatures, and results in a total number of phases much lower than the maximum equilibrium number allowed by the Gibbs phase rule.

3.7. Vicker hardness

Figure 9 shows the Vicker hardness values according to the annealing regime. It can be seen that the hardness gradually increases during annealing at 600ºC, 700ºC, and 825ºC and reaches a maximum value of ~ 614 kg/mm^2 at 600ºC/24 hours, which is entirely consistent with the obtained microstructure morphology.

The hardness increases because the morphology of the dendrite phase becomes more equiaxial, and the distance between these phases decreases with increasing annealing time. In addition, the distribution of the interdendritic phase is more uniform, and precipitate phases likely play an essential role in increasing the hardness of the alloy. The precipitate phases likely play a significant role in increasing the alloy's hardness. The hardness remained almost constant when annealed at 925ºC for 8 and 16 hours but decreased rapidly when the time was increased to 24 hours. The hardness then decreased continuously with increasing annealing time at 1000ºC. The results of the last two cases can be expected due to the rapid coarsening of the dendritic phase, the decrease in the proportion of the excreted phase in the alloy, and the appearance of plastic flow phenomena at grain boundaries.

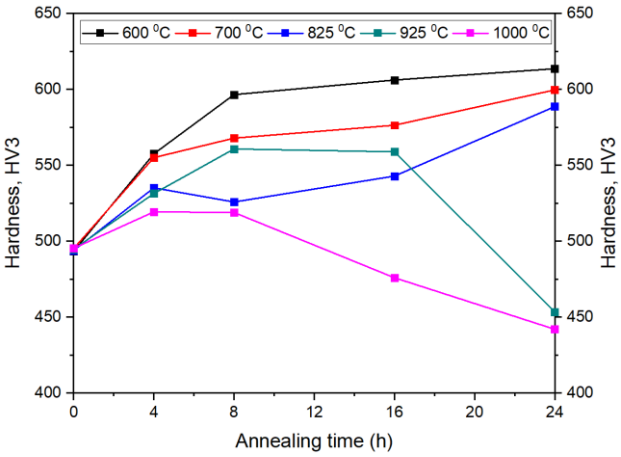

Fig. 9. HV3 hardness of samples after annealing in different regimes.

4. Conclusions

The dendritic phase in the as-cast state can be up to hundreds of µm, transforming into a more equiaxial phase that decreases in size. The interdendritic phase is more evenly distributed, and its proportion increases with increasing annealing temperature.

Annealing temperature and time significantly affect the alloy's precipitation process. The precipitate phase begins to appear when annealing is carried out at 700ºC for 8 hours; this process occurs earlier when the annealing temperature is increased above 825ºC. However, the precipitate phase gradually disappears at 1000ºC for 24 hours.

The alloy's hardness undergoes significant variations based on the proportion of the precipitate phase in the microstructure. This relationship underscores the practical implications of our research, as it demonstrates the direct link between microstructure and properties.

Acknowledgement

This research is funded by Le Quy Don Technical University Research Fund under the grant number 24.1.14.

References

[1] J. W. Yeh, S. K. Chen, S. J. Lin *et al.*, "Nanostructured high-entropy alloys with multiple principal elements: Novel alloy design concepts and outcomes", *Advanced Engineering Materials*, Vol. 6, Iss. 5, pp. 299-303, 2004. DOI: 10.1002/adem.200300567

[2] J. W. Yeh, S. J. Lin, T. S. Chin *et al.*, "Formation of simple crystal structures in Cu-Co-Ni-Cr-Al-Fe-Ti-V alloys with multiprincipal metallic elements", *Metallurgical and Materials Transactions A*, Vol. 35, Iss. 8, pp. 2533-2536, 2004. DOI: 10.1007/s11661-006-0234-4

[3] O. N. Senkov, G. B. Wilks, J. M. Scott, and D. B. Miracle, "Mechanical properties of $Nb_{25}Mo_{25}Ta_{25}W_{25}$ and $V_{20}Nb_{20}Mo_{20}Ta_{20}W_{20}$ refractory high entropy alloys", *Intermetallics*, Vol. 19, Iss. 5, pp. 698-706, 2011. DOI: 10.1016/j.intermet.2011.01.004

[4] A. Gali and E. P. George, "Tensile properties of high- and medium-entropy alloys", *Intermetallics*, Vol. 39, pp. 74-78, 2013. DOI: 10.1016/j.intermet.2013.03.018

[5] F. Otto, A. Dlouhý, Ch. Somsen *et al.*, "The influences of temperature and microstructure on the tensile properties of a CoCrFeMnNi high-entropy alloy", *Acta Materialia*, Vol. 61, Iss. 15, pp. 5743-5755, 2013. DOI: 10.1016/j.actamat.2013.06.018

[6] O. N. Senkov, S. V. Senkova, D. B. Miracle, and C. Woodward, "Mechanical properties of low-density, refractory multi-principal element alloys of the Cr–Nb–Ti–V–Zr system", *Materials Science and Engineering: A*, Vol. 565, pp. 51-62, 2013. DOI: 10.1016/j.msea.2012.12.018

[7] C. Suryanarayana, "Mechanical alloying: A novel technique to synthesize advanced materials", *Research*, Vol. 2019, 2019. DOI: 10.34133/2019/4219812

[8] M. R. Chen, S. J. Lin, J. W. Yeh *et al.*, "Effect of vanadium addition on the microstructure, hardness, and wear resistance of $Al_{0.5}$CoCrCuFeNi high-entropy alloy", *Metallurgical and Materials Transactions A*, Vol. 37, pp. 1363-1369, 2006. DOI: 10.1007/s11661-006-0081-3

[9] Y. P. Wang, B. S. Li, and H. Z. Fu, "Solid solution or intermetallics in a high-entropy alloy", *Advanced Engineering Materials*, Vol. 11, Iss. 8, pp. 641-644, 2009. DOI: 10.1002/adem.200900057

[10] Y. L. Chou, J. W. Yeh, and H. C. Shih, "The effect of molybdenum on the corrosion behaviour of the high-entropy alloys $Co_{1.5}CrFeNi_{1.5}Ti_{0.5}Mo_x$ in aqueous environments", *Corrosion Science*, Vol. 52, Iss. 8, pp. 2571-2581, 2010. DOI: 10.1016/j.corsci.2010.04.004

[11] M. H. Chuang, M. H. Tsai, W. R. Wang, S. J. Lin, and J. W. Yeh, "Microstructure and wear behavior of Al$_x$Co$_{1.5}$CrFeNi$_{1.5}$Ti$_y$ high-entropy alloys", *Acta Materialia*, Vol. 59, Iss. 16, pp. 6308-6317, 2011. DOI: 10.1016/j.actamat.2011.06.041

[12] S. Singh, N. Wanderka, B. S. Murty, U. Glatzel, and J. Banhart, "Decomposition in multi-component AlCoCrCuFeNi high-entropy alloy", *Acta Materialia*, Vol. 59, Iss. 1, pp. 182-190, 2011. DOI: 10.1016/j.actamat.2010.09.023

[13] W. R. Wang, W. L. Wang, S. C. Wang *et al.*, "Effects of Al addition on the microstructure and mechanical property of Al_xCoCrFeNi high-entropy alloys", *Intermetallics*, Vol. 26, pp. 44-51, 2012. DOI: 10.1016/j.intermet.2012.03.005

[14] F. Otto, Y. Yang, H. Bei, and E. P. George, "Relative effects of enthalpy and entropy on the phase stability of equiatomic high-entropy alloys", *Acta Materialia*, Vol. 61, Iss. 7, pp. 2628-2638, 2013. DOI: 10.1016/j.actamat.2013.01.042

[15] D. G. Shaysultanov, N. D. Stepanov, A. V. Kuznetsov, G. A. Salishchev, and O. N. Senkov, "Phase composition and superplastic behavior of a wrought AlCoCrCuFeNi high-entropy alloy", *JOM*, Vol. 65, pp. 1815-1828, 2013. DOI: 10.1007/s11837-013-0754-5

[16] J. W. Yeh, "Alloy design strategies and future trends in high-entropy alloys", *JOM*, Vol. 65, pp. 1759-1771, 2013. DOI: 10.1007/s11837-013-0761-6

[17] J. Y. He, W. H. Liu, H. Wang *et al.*, "Effects of Al addition on structural evolution and tensile properties of the FeCoNiCrMn high-entropy alloy system", *Acta Materialia*, Vol. 62, pp. 105-113, 2014. DOI: 10.1016/j.actamat.2013.09.037

[18] G. A. Salishchev, M. A. Tikhonovsky, D. G. Shaysultanov *et al.*, "Effect of Mn and V on structure and mechanical properties of high-entropy alloys based on CoCrFeNi system", *Journal of Alloys and Compounds*, Vol. 591, pp. 11-21, 2014. DOI: 10.1016/j.jallcom.2013.12.210

[19] Y. Zhang, T. Zuo, Z. Tang *et al.*, "Microstructures and properties of high-entropy alloys", *Progress in Materials Science*, Vol. 61, pp. 1-93, 2014. DOI: 10.1016/j.pmatsci.2013.10.001

[20] S. G. Ma and Y. Zhang, "Effect of Nb addition on the microstructure and properties of AlCoCrFeNi high-entropy alloy", *Materials Science and Engineering: A*, Vol. 532, pp. 480-486, 2012. DOI: 10.1016/j.msea.2011.10.110

[21] H. Jiang, L. Jiang, D. Qiao *et al.*, "Effect of niobium on microstructure and properties of the $CoCrFeNb_xNi$ high entropy alloys", *Journal of Materials Science & Technology*, Vol. 33, Iss. 7, pp. 712-717, 2017. DOI: 10.1016/j.jmst.2016.09.016

[22] G. Qin, Z. Li, R. Chen *et al.*, "CoCrFeMnNi high-entropy alloys reinforced with Laves phase by adding Nb and Ti elements", *Journal of Materials Research*, Vol. 34, Iss. 6, pp. 1011-1020, 2019. DOI: 10.1557/jmr.2018.468

[23] N. Malatji, A. P. I. Popoola, T. Lengopeng, and S. Pityana, "Effect of Nb addition on the microstructural, mechanical and electrochemical characteristics of AlCrFeNiCu high-entropy alloy", *International Journal of Minerals, Metallurgy and Materials*, Vol. 27, pp. 1332-1340, 2020. DOI: 10.1007/s12613-020-2178-x

[24] X. Yang and Y. Zhang, "Prediction of high-entropy stabilized solid-solution in multi-component alloys", *Materials Chemistry and Physics*, Vol. 132, Iss. 2-3, pp. 233-238, 2012. DOI: 10.1016/j.matchemphys.2011.11.021

[25] K. Zhang and Z. Fu, "Effects of annealing treatment on phase composition and microstructure of $CoCrFeNiTiAl_x$ high-entropy alloys", *Intermetallics*, Vol. 22, pp. 24-32, 2012. DOI: 10.1016/j.intermet.2011.10.010

[26] V. S. Hariharan, A. Karati, T. Parida *et al.*, "Effect of Al addition and homogenization treatment on the magnetic properties of CoFeMnNi high-entropy alloy", *Journal of Materials Science*, Vol. 55, pp. 17204-17217, 2020. DOI: 10.1007/s10853-020-05171-8

[27] J. Xu, J. Y. Zhang, Y. Q. Wang *et al.*, "Annealing-dependent microstructure, magnetic and mechanical properties of high-entropy $FeCoNiAl_{0.5}$ alloy", *Materials Science and Engineering: A*, Vol. 776, 2020, 139003. DOI: 10.1016/j.msea.2020.139003

[28] C. Yang, J. Zhang, M. Li, and X. Liu, "Soft-magnetic high-entropy AlCoFeMnNi alloys with dual-phase microstructures induced by annealing", Acta Metallurgica Sinica (English Letters), Vol. 33, pp. 1124-1134, 2020. DOI: 10.1007/s40195-020-01086-0

[29] H. Cheng, H. Luo, X. Wang, and X. Li, "Microstructure and corrosion resistance properties of $(FeCoNi)_{86}Al_7Ti_7$ high-entropy alloy via different aging time", *Corrosion Science*, Vol. 226, 2024, 111670. DOI: 10.1016/j.corsci.2023.111670

[30] S. Guo, C. P. Ng, J. Lu, and C. T. Liu, "Effect of valence electron concentration on stability of FCC or BCC phase in high entropy alloys", *Journal of Applied Physics*, Vol. 109, 2011. DOI: 10.1063/1.3587228

[31] X. Tan, Y. Tang, Y. Tan *et al.*, "Correlation between microstructure and soft magnetic parameters of Fe-Co-Ni-Al medium-entropy alloys with FCC phase and BCC phase", *Intermetallics*, Vol. 126, 2020, 106898. DOI: 10.1016/j.intermet.2020.106898

ẢNH HƯỞNG CỦA CHẾ ĐỘ Ủ ĐẾN SỰ TIẾT PHA CỦA HỢP KIM ENTROPY CAO $FeCoNiAl_{0,75}Nb_{0,25}$

Lê Minh Đức[1,2], Nguyễn Thanh Hùng[1], Nguyễn Mạnh Hùng[1], Nguyễn Hồng Hải[2]

[1]*Khoa Cơ khí, Trường Đại học Kỹ thuật Lê Quý Đôn*

[2]*Trường Vật liệu, Đại học Bách Khoa Hà Nội*

Tóm tắt: Bài báo này nghiên cứu ảnh hưởng của chế độ ủ đến sự tiết pha của hợp kim entropy cao $FeCoNiAl_{0,75}Nb_{0,25}$. Cấu trúc vi mô sau đúc bao gồm các pha nhánh cây thô, to được thay thế bằng hình thái đẳng trục, và sự phân bố của pha giữa nhánh cây trở nên đồng đều hơn khi tăng thời gian và nhiệt độ ủ lên tới 825°C. Quá trình tiết pha bắt đầu ở 700°C trong 8 giờ, thời gian tiết pha được rút ngắn xuống 4 giờ khi tăng nhiệt độ ủ. Kích thước của pha này chỉ vài µm. Tỉ lệ pha tiết ra tăng và kích thước của pha nhánh cây giảm khi nhiệt độ ủ tiến tới 825°C, trong khi kích thước này tăng ở chế độ 925°C/16 giờ. Cấu trúc vi mô thô, pha tiết ra dần biến mất khi ủ ở 1000ºC. Độ cứng HV3 của hợp kim tăng theo thời gian khi nhiệt độ thấp hơn 825ºC và đạt giá trị cao nhất ~ 614 kg/mm^2 ở 600ºC/24 giờ; giá trị này bắt đầu giảm ở chế độ 925°C/16 giờ. Trong khi đó, độ cứng giảm dần khi tăng thời gian ủ ở 1000°C. Có thể dự đoán là do sự thô hóa nhanh của pha nhánh cây, tỉ lệ pha tiết ra trong hợp kim giảm và xuất hiện hiện tượng chảy dẻo ở biên giới hạt.

Từ khóa: *Hợp kim entropy cao; hợp kim $FeCoNiAl_{0,75}Nb_{0,25}$; quá trình ủ; tiết pha.*

Received: 28/07/2024; Revised: 30/09/2024; Accepted for publication: 30/10/2024

❑